Available online at www.sciencedirect.com
ScienceDirect
Journal of the European Ceramic Society 30 (2010) 1211–1221
www.elsevier.com/locate/jeurceramsoc

Review

Densification and microstructure evolution of Y-Tetragonal Zirconia Polycrystal powder during direct and hybrid microwave sintering in a single-mode cavity

Sylvain Charmond, Claude Paul Carry, Didier Bouvard *

SIMaP, Grenoble Institute of Technology, Université Joseph Fourier, CNRS, BP 75, F-38 402 St-Martin d'Hères, France

Received 1 July 2009; received in revised form 4 November 2009; accepted 26 November 2009
Available online 19 January 2010

Abstract

The densification and microstructure changes of 2 mol% yttria-stabilized zirconia nanopowder have been investigated during direct and hybrid microwave sintering. Microwave heating tests were achieved in a resonant single-mode cavity at 2.45 GHz and a cylindrical SiC susceptor was used for hybrid sintering experiments. Constant heating rate runs (25 °C/min) were controlled by adjusting the position of a sliding piston at constant forward microwave power. The temperature on the upper surface of the specimen was measured with an infrared camera. The final densities and the microstructures observed by SEM were compared to those of conventionally sintered materials. Homogeneous microstructures have been obtained by hybrid heating whereas direct microwave heating led to rather heterogeneous microstructures due to thermal gradients. Nevertheless, microwave-sintered materials always exhibited higher final densities for a given sintering temperature. This significant enhancement of the densification process was particularly observed in the intermediate sintering stage (1200–1350 °C range). Besides, grain growth was found to be mainly influenced by the sintering temperature rather than by the heating mode.

Keywords: Microwave processing; Sintering; Grain size; Microstructure; ZrO_2

Contents

* Corresponding author. Tel.: +33 476 82 63 07; fax: +33 476 82 63 82.
E-mail address: didier.bouvard@grenoble-inp.fr (D. Bouvard).

0955-2219/$ – see front matter © 2009 Elsevier Ltd. All rights reserved.
doi:10.1016/j.jeurceramsoc.2009.11.014

1. Introduction

Microwave heating of dielectric materials, such as ceramics, results from the absorption by molecular vibration (rotating electric dipole/dipole reorientation) and ionic conduction of a portion of the energy transported by an oscillating electric field.[1,2] It has been shown that most ceramic powders can be sintered by microwave at lower temperatures and for shorter times than in conventional sintering, which allows for finer and more uniform microstructures to be obtained.[3–7] A genuine "microwave effect", i.e. the acceleration of diffusion mechanisms by the oscillating electric field, was also proposed by some authors to explain the enhancement of the sintering process.[6,8–11] However, clear evidence of such an effect has not been given so far, due to the difficulty of comparing microwave and conventional sintering in perfectly identical thermal conditions.

Due to its specific dielectric properties and its wide range of applications, microwave sintering of yttria-doped zirconia has been extensively studied in various types of microwave furnaces. Yttria-doped zirconia powder shows poor coupling with the microwaves below 400 °C and moderate coupling above. Thus, most published studies have used hybrid heating devices such as multimode cavities with SiC rods,[6,8,9,12,13] or a thin layer of SiC powder[10] acting as a susceptor, or microwave/conventional hybrid furnaces.[11,14] Noteworthy is the study of Goldstein et al.[15] where specimens were sintered by direct microwave heating. A more limited amount of works involved single-mode cavity. The use of a SiC plate[16], a $ZnO–MnO_2–Al_2O_3$ plate[17] or a SiC tube susceptor[18] allowed long warming-up time before the coupling of the material. Besides, the presintering of the material and the employment of an adjustable iris allowing for a resonance mode[5] have been found to be necessary for direct microwave sintering in a single-mode cavity. All these microwave cavities included different types of insulating devices to limit radiative loss out of the materials. Miscellaneous techniques have been proposed to measure the temperature of the material: thermocouple, optical or IR pyrometer and thermal imaging camera. The diversity of experimental procedures and conditions makes for a difficult overview of the behaviour of zirconia powder during microwave sintering. This is particularly true for the response of zirconia powder to a pure electric field. Nevertheless, significant results, mainly on zirconia powders with low yttria content (2 mol% or 3 mol%), have been obtained (i) in single-mode cavities and (ii) in multimode cavities. These results are summarized below.

(i) Several authors have noted the potential of single-mode cavity microwave heating[5,16] in maintaining a nanometric grain size in densified specimens, owing to much shorter sintering times than those required for conventional heating. However, smaller grain size was not achieved when microwave heating was used for sintering. Also, Wilson and Kunz[16] used a silicon carbide plate susceptor since direct microwave heating was not possible in their non-resonant cavity due to a lack of plunger or of a coupling iris. Tian[5] claimed that the production of uncracked parts was not possible without a presintering step (1 h at 1150 °C in his study), which transforms the residual monoclinic phase into a tetragonal phase. Such presintering step is not necessary for nanometric or fully stabilized zirconia powders.

(ii) Hybrid microwave sintering experiments at low heating rate (2 °C/min) in multimode cavity evidenced a larger densification (as compared to conventional heating) for a given sintering temperature and a smaller grain size for the same final density.[8] This is true below 96% of relative density. These results have been attributed by the authors to an acceleration of lattice diffusion compared to surface and grain-boundary diffusions during the initial and intermediate stages of sintering. Moreover, ageing experiments conducted at 1500 °C showed that once densification was near completion, grain growth was accelerated in the microwave field and exaggerated grain growth occurred.[9] However, in this study, the temperature was measured by a thermocouple located in the cavity and thus was in all likelihood lower than the temperature in the bulk of the material. An interesting result was obtained by Binner et al.[14] on a 3 mol% yttria partially stabilized zirconia nanopowder in their innovative hybrid microwave/conventional furnace. By combining hybrid heating with the two stage sintering technique developed by Chen and Wang,[19] these authors obtained nearly fully dense material (>99%) with a very fine grain size in the range 60–80 nm. Finally, Goldstein et al.[15] obtained by direct microwave sintering uncracked specimens from an yttria-doped zirconia powder containing monoclinic phase and without preliminary thermal treatment. They thus showed that starting from room temperature microwave sintering was feasible without using any susceptor in a multimode applicator. However they were not able to keep a constant heating rate in the 400–1000 °C range and, as most other authors, they did not report detailed information on the microstructure homogeneity.

In spite of the large number of publications on popular commercial Tosoh Y-TZP powders, the mechanisms controlling the conventional sintering of such Tetragonal Zirconia Polycrystals have not been thoroughly studied and are still largely controversial. Most studies[20] have tried to correlate the apparent activation energies to the activation energy of grain-boundary diffusion of Zr^{4+} ions, which has been estimated at 310 kJ/mol for a cubic zirconia polycrystal stabilized with yttria. Recently Bernard-Granger and Guizard[21] reported that the apparent activation energy of 3Y-TZP powder densification decreased from 935 kJ/mol to 310 kJ/mol as the relative density increased from 0.68 to 0.92 and as the grain size increased from 120 nm to 170 nm. According to them, the 935 kJ/mol value proves that the limiting mechanism at low relative density and for small grain size is not diffusion but point defect formation (also defined as "interface reaction" in creep studies). This interpretation means that it is more difficult to create a point defect at grain surfaces than at grain boundaries and that diffusion distances are too short in such nanometric microstructures for the diffusion to be a limiting phenomenon. A second specific behaviour of Y-TZP powder during conventional sintering is its restricted grain

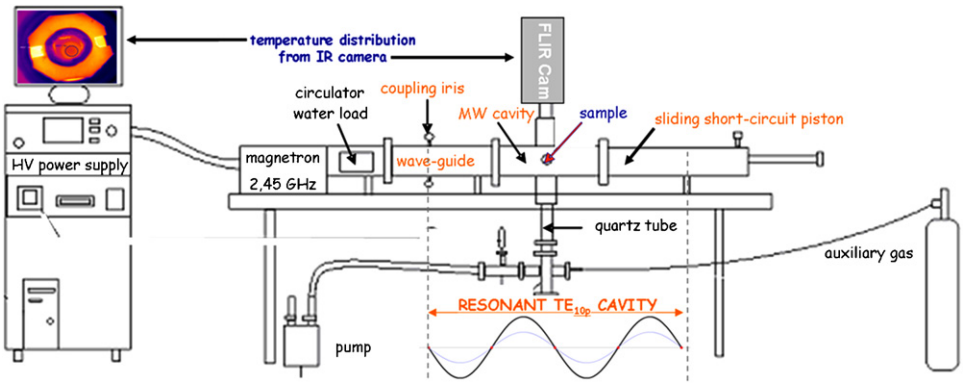

Fig. 1. Schematic of the single-mode microwave furnace.

growth at high density, which has been called "sluggish grain growth" in the literature.[22] This has been attributed to a solute drag effect of Y^{3+} ions segregating at the grain boundaries during the phase partitioning process.

The present study aim is to contribute to the understanding of the specific effects of electric field on the densification and microstructure changes of zirconia nanomaterials. For this purpose, we chose a 2 mol% yttria-doped zirconia nanopowder. A rectangular single-mode cavity at 2.45 GHz instrumented with a thermal imaging camera was used. This device has been designed to study either direct or susceptor-assisted microwave sintering of various kinds of ceramic and metal powders under separated electric or magnetic field. In this paper, direct microwave heating experiments under electric field have been compared to hybrid microwave heating and conventional sintering experiments with identical thermal cycle. During microwave processing, the heating rate was controlled by changing the position of a movable reflector to yield the desired temperature–time profile. The specimen temperature and the power dissipated in the cavity were recorded during sintering. The microstructure of sintered materials has been observed in different zones of the specimens and the corresponding average grain sizes have been evaluated. Building on the comparison of the grain sizes and of the density of direct microwave, hybrid microwave and conventionally sintered specimens, the effectiveness and the specific effects of the electric field are shown and their interpretation in terms of sintering mechanisms are discussed.

2. Experiments

2.1. Microwave system setup

The experimental setup is schematized in Fig. 1. It includes a high voltage power supply (microwave generator SAIREM GMP 20KSM, France) linked to a magnetron that delivers a variable forward power of up to 2 kW at 2.45 GHz. A rectangular wave-guide of 86.36 mm × 43.18 mm section allows for the transport of the microwave radiation to a rectangular TE_{10p} cavity.[23] This resonant cavity is closed by a coupling iris (a vertical slot in a copper sheet) on the magnetron side and by a reflector on the other side.

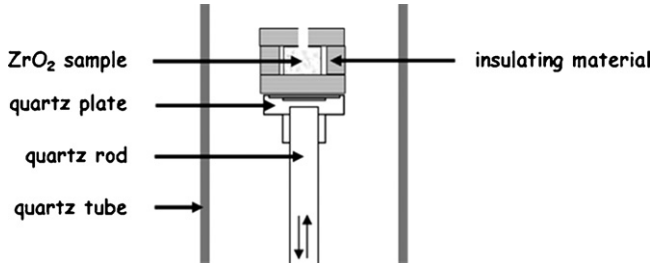

Fig. 2. Sample surroundings during direct microwave sintering.

Samples are located inside a vertical 40 mm-diameter quartz tube that crosses the cavity. They are set upon a quartz plate and are surrounded by an alumina fibreboard box for thermal insulation, as shown in Fig. 2. In the case of hybrid sintering (Fig. 3), a cylindrical SiC susceptor (internal diameter: 20 mm; height: 15 mm; thickness: 5 mm) is placed around the compact and insulating materials are located only below and above the specimen. The temperatures of the upper surfaces of the specimen and of the susceptor are continuously measured by an IR camera (FLIR SYSTEMS, ThermoVision™ A40 M, Sweden), which is located 14 cm above the middle of the cavity and is protected by a ZnSe window. This camera converts infrared radiation from the surfaces facing it into an image that depicts temperature variations across these surfaces. A software correlates a temperature value to each pixel of this image and can also calculate average values in prescribed zones of the image. A necessary input is the emissivity of the surfaces, which may be difficult to evaluate with accuracy, in particular at high temperature. Calibration experiments have thus been performed in a conventional furnace

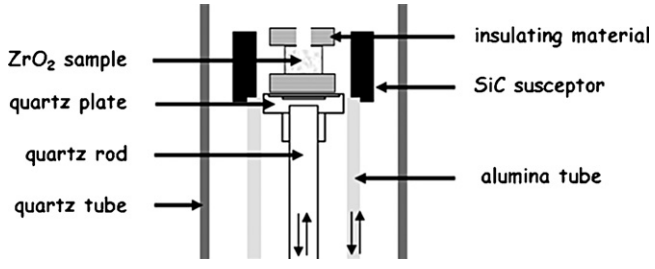

Fig. 3. Sample surroundings during hybrid microwave sintering.

to estimate the emissivity of zirconia and silicon carbide in the relevant temperature range. In the analysis of microwave sintering tests, the temperature of the specimen was chosen to be the average temperature of the portion of the specimen surface that is seen by the camera through a small hole drilled in the cap of the insulating material (see Figs. 2 and 3). The temperature of the susceptor was defined as the average temperature of its upper surface. Taking into account all causes of uncertainty and the inaccuracy on emissivity measurement, the precision on temperature measurement has been estimated as ±10 °C.

All along the test, we also measured the input power delivered by the magnetron (forward power) and the output power leaving the cavity (reflected power). The dissipated powder has been defined as the difference between the input and output powers. It includes the power required to heat the specimen and various losses (coupling of microwaves with the walls of the cavity and the specimen support and heat transfer from the surface of the specimen). For further analysis it is useful to note that the power required to heat a 1 g zirconia specimen at 25 °C/min is less than 1 W.

During microwave heating, the forward electromagnetic wave is reflected against the conductive wall of the short-circuit piston, leading to a standing wave made of a single stacking of forward and reflected waves. In the empty cavity, the distance between points where the magnetic and electric fields are respectively maximum and minimum (near to zero) is equal to a quarter of the guided wave-length (43 mm). Besides, when the iris–piston distance (cavity length) is equal to 4 or 5 times the half guided wave-length, the iris reflects almost entirely the wave in the cavity (TE_{104} or TE_{105} resonant mode). The resonance phenomenon consists in the stacking of multiple waves reflected against the piston and the iris, which results in an increase of the electromagnetic energy in the cavity. In our cavity, the TE_{104} and the TE_{105} resonant modes are used for materials interacting respectively with the magnetic field or with the electric field. Since ceramic materials, such as yttria-doped zirconia, are supposed to interact with the electric field, the specimens should be located where the electric field is maximum, i.e. in the centre of the cavity in the TE_{105} mode. However, when materials are located in the cavity (specimen, quartz and alumina holders, insulating materials, susceptor, etc.) the electromagnetic pattern is modified. Thus, the cavity length (iris–piston distance) of the resonant mode TE_{10p} is also modified. It is about 440 mm with the direct microwave configuration and it is only in the 400–405 mm range with the hybrid microwave configuration, instead of 432 mm in the empty cavity. In our setup, the coupling iris and the specimen were fixed during an experiment whereas the position of the sliding short-circuit piston was adjusted continuously. Ideally, the iris–specimen distance should be chosen to be approximately equal to half of the cavity length leading to a resonant mode. This allows for the best coupling between the material and the electric field at resonance (maximum dissipated power). Nevertheless, we observed in preliminary runs that this optimal position resulted in overheating and cracking of the specimen during the early stage of sintering. Thus, in order to follow the prescribed thermal cycle and secondarily to avoid cracking, we chose to continuously adjust the position of the piston during the test so that the cavity got at any time the electromagnetic power required to heat the specimen at a specified rate. It means that we did not stick to the position that was the most favourable to specimen heating.

2.2. Experimental procedure

The raw material is a spray-dried 2 mol% yttria-doped zirconia powder manufactured by Tosoh. Its BET specific area is 16 m^2/g and the resultant equivalent BET particles size is 60 nm. SEM observation showed that the zirconia grains were agglomerated in 10–80 μm sized aggregates of spherical shape. Green samples were prepared in two steps for a better control of the specimen cylindrical shape. Uniaxial pressing (UP) at low pressure (50 MPa) in a cylindrical die was first carried out. It was then followed by cold isostatic pressing at 250 MPa. The green density was approximately 2.9 g/cm^3, i.e. 48% of theoretical density (6.05 g/cm^3). Before sintering, the binder was burnt out under air in an electric furnace by heating at 5 °C/min up to 600 °C and by soaking for 3 h. The weight loss was about 0.5%. This preliminary debinding stage is necessary, since we observed crack development during microwave heating for other specimens. This is due to a very heterogeneous temperature distribution, as already mentioned by Janney et al.[6]

Green samples were sintered by direct microwave heating, by susceptor-assisted hybrid microwave heating in the previously described setup, or by conventional heating in a vertical dilatometer (LINSEIS L75/1550, Germany). The bulk density of the sintered samples was measured by Archimedes' principle by immersing the sample into an ethanol based liquid. Sintered samples were longitudinally cut in half cylinders with a diamond saw. Polished sections were thermally etched between 20 min and 30 min in an electrical furnace under air 50 °C below their maximal sintering temperature to reveal their microstructure. These sections have been observed using a field emission gun scanning electron microscope (FEG-SEM—Secondary Electrons detector) and the average grain size was determined from SEM micrographs by a surface intercept method ($d = 1.38\sqrt{s}$, where s is the intercepted surface of grains). The comparison of micrographs of fracture surfaces before and after thermal etching showed that the grain size may noticeably increase during thermal etching. However, since the grain size cannot be precisely evaluated from fracture surface micrographs, we used the data obtained from etched surfaces. One should keep in mind that the values of grain size given below are overestimated. We assume that such systematic bias does not change the main conclusions of our analysis.

In the following, 11 sintering experiments will be described[2] and analyzed: three conventional sintering tests (C), three direct microwave sintering runs (D) and five hybrid microwave sintering runs (H). Table 1 provides the forward microwave power (FP), the heating rate, the maximum sintering temperature, the final relative density (percentage of theoretical density) and the average grain size for each test. Note that the compacts had almost the same sizes, 7.35 ± 0.05 mm in diameter, 7.95 ± 0.10 mm in height, 0.99 ± 0.01 g in weight. The final densities and grain sizes will be discussed in Section 3.

Table 1
Miscellaneous data on sintering experiments.

Name	FP (W)	Sintering temperature (°C)	Density (g/cm^3)	Relative density (%TD)	Average grain size (nm)
Conventional sintering—2 °C/min					
C0	–	1550	6.05	100.0	450
Conventional sintering—25 °C/min					
C1	–	1360	5.53	91.4	220
C2	–	1550	5.74	94.8	430
Direct microwave sintering—25 °C/min					
D3	500	1275	5.75	95.1	200–250
D4	500	1360	5.75	95.0	240–270
D5	500	1500	5.86	96.8	380–450
Hybrid microwave sintering—25 °C/min					
H6	1000	1200	4.89	80.7	120–140
H7	1000	1275	5.48	90.5	140–190
H8	1000	1340	5.80	95.8	210–230
H9	1000	1350 (1 h)	5.96	98.6	230–270
Hybrid microwave sintering—250 °C/min					
H10	1000	1225	5.26	86.9	130–180

2.3. Direct microwave sintering

During direct microwave sintering tests, the forward power was fixed to 500 W and the iris–specimen distance was 215 mm. We aimed at maintaining a constant heating rate of 25 °C/min from room temperature to about 1500 °C by adjusting the position of the short-circuit piston. As an example, the temperature of the upper surface of the sample and the dissipated power measured during the D5 test have been plotted in Fig. 4. The required heating cycle was correctly followed up to 1500 °C. At low temperature, the dissipated power slightly increased up to 60 W and remained almost constant until 400 °C. Next, the dissipated power decreased and remained under 50 W while the temperature of the specimen continued to increase up to 1100 °C. The heating rate was difficult to control in the 400–1000 °C range due to the sharp change of the dielectric parameters (permittivity, loss tangent[24]) of zirconia, as illustrated by the sudden variation of zirconia temperature (red curve) compared to the reference thermal cycle (blue line). Above this temperature, the dissipated power increased steadily and attained 150 W when the temperature reached 1500 °C. Finally, the forward power was cut off for cooling. D3 and D4 tests exhibited about the same features, except that the maximal temperature was respectively 1275 °C and 1360 °C.

The variations of the dissipated power throughout sintering can be explained as follows. Firstly, it is important to note that the measured power is much larger than the power required to heat the specimen, which is less than 1 W, as already mentioned. It means that the dissipated power is almost entirely due to losses within the cavity components and out of the specimen. At low temperature, when the coupling between the zirconia powder and the microwaves is poor, the electric field in the cavity should be high so that the powder can heat at the prescribed rate. Then, the piston was positioned close to the position leading to

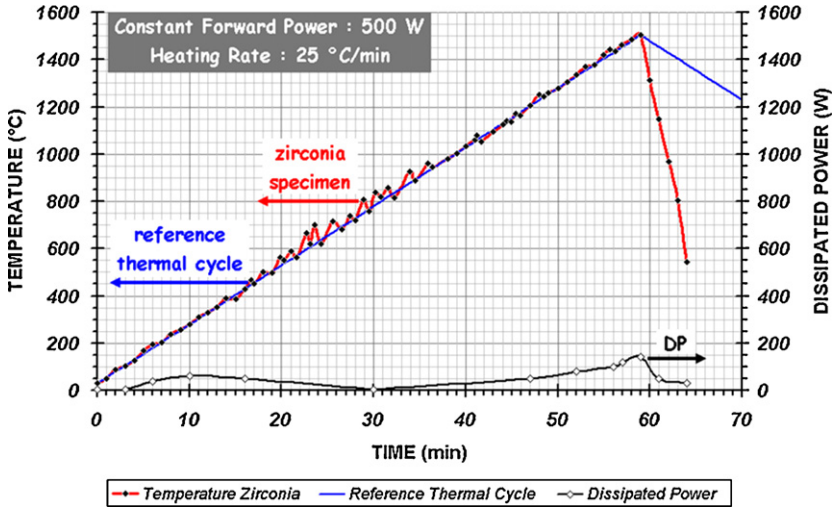

Fig. 4. Evolution of the temperature and the dissipated power during direct microwave sintering run (D5).

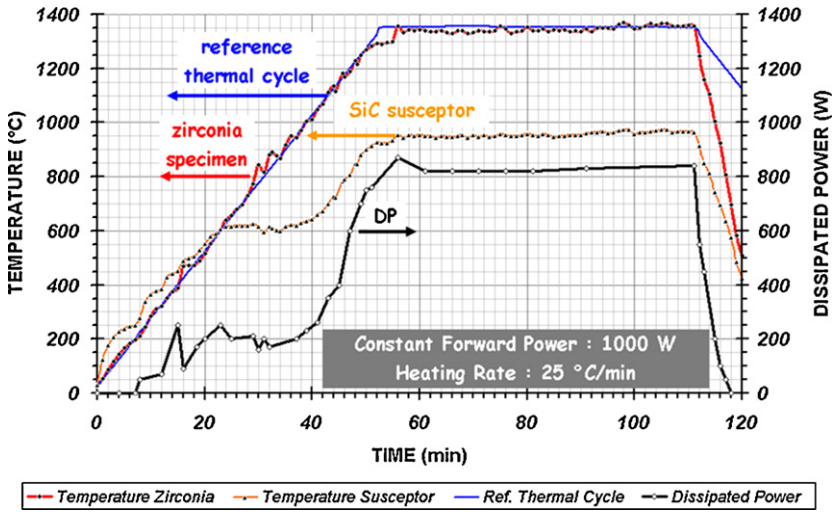

Fig. 5. Evolution of specimen and susceptor temperatures and of the dissipated power during hybrid microwave sintering run (H9).

resonance. As a consequence of a high electric field, the losses in the cavity and the dissipated power were significant. When the specimen started to couple with the microwaves, the electric field was decreased by moving the piston, so that the heating rate did not pass the aimed value. Hence the dissipated power resulting from losses in the cavity got lower. When the temperature T increased, the losses out of the specimen, which were mainly radiative, became larger and larger. The dissipated power increased accordingly.

2.4. Hybrid microwave sintering

During hybrid runs, the distance between the iris and the specimen was set to 202 mm. In each test (except H10), a heating rate of 25 °C/min was applied from room temperature to the sintering temperature by adjusting the position of the movable reflector with 1000 W constant forward power. The maximum temperatures were 1200 °C, 1275 °C, 1340 °C and 1350 °C in H6, H7, H8 and H9 runs, respectively. For example, Fig. 5 shows the variation of the parameters recorded during the H9 test, which included a 1 h soaking period at 1350 °C. From room temperature to 600 °C, the specimen remained cooler than the SiC susceptor due to its poorer dielectric properties (smaller loss tangent) at low temperature. Therefore, zirconia was mainly heated by thermal radiance from the susceptor. Above 600 °C, the specimen became hotter than the susceptor; its temperature followed more or less the prescribed thermal cycle from 600 °C to 1000 °C whereas the temperature of the susceptor remained approximately constant at 600 °C. We thus infer that the compact was heated by both radiance from the susceptor and by coupling with the microwaves (hybrid heating). The dissipated power varied in the 150–250 W range. Above 1000 °C, the dissipated power sharply increased to 850 W and the temperature reached 1350 °C at the upper surface of the zirconia specimen and only 950 °C in the susceptor. Note that the SiC susceptor did not cool off contrary to the observation of Wilson and Kunz[16] or Janney et al.[6] All parameters remained almost constant during the soaking time. It is noteworthy that the temperature of the susceptor and the dissipated power show similar time variations. Also we observe that the value of the dissipated power is

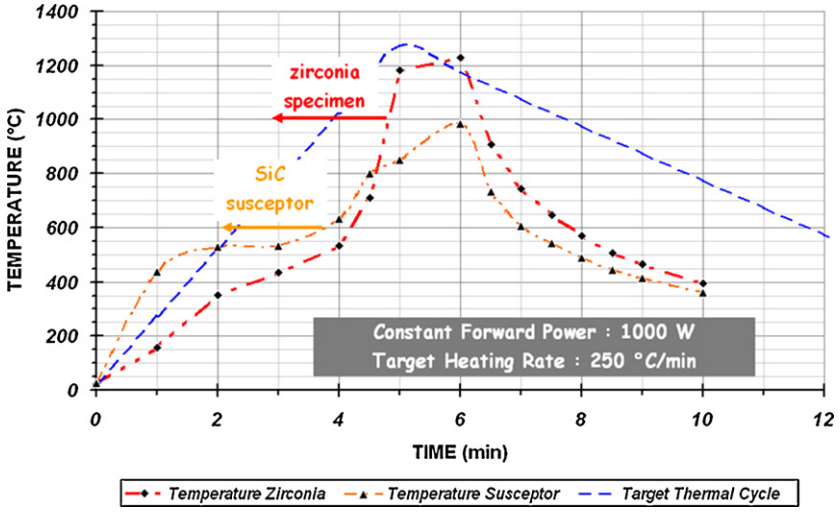

Fig. 6. Evolution of specimen and susceptor temperatures during fast hybrid microwave sintering run (H10).

much larger than the one measured during direct microwave sintering runs. The dissipated power difference, especially above 650 °C, is due to the heating and to the radiative losses of the SiC susceptor set in the cavity so as to perform hybrid microwave sintering.

With H10 hybrid run (presented in Fig. 6), we considered the possibility of achieving much faster heating with our device and we investigated the effect of such high heating rate on microstructure evolution. The specimen was heated from room temperature to 1200 °C in 5 min (average heating rate: 200 °C/min) and the total processing time was about 10 min including cooling. The susceptor reached a temperature of 980 °C, i.e. slightly above the temperature of the previous tests. Note that the control of the heating rate was very poor as we could not avoid overheating periods. We assume that this is due to the strong changes in dielectric properties of zirconia between 400 °C and 1000 °C.

3. Results: characterization of sintered materials

3.1. Final density

The final relative density of the specimens sintered during the experiments previously presented is plotted in Fig. 7 as a function of their maximal sintering temperature. In the following discussion, the reference data will be the curve relating the relative density to the temperature from the results of conventional sintering tests at 25 °C/min. The relative density of this test has been calculated from the axial shrinkage measured continuously by the dilatometer and from the density of the sintered specimen with the assumption of isotropic shrinkage. This assumption is reasonable since the final specimen showed isotropic shrinkage. The black plain curve depicts the continuous changes of the relative density vs. the temperature for the conventional test C2, which has been obtained with the same procedure. The C1 and C2 conventional runs reached relative densities of 91.4% at 1360 °C and 94.8% at 1500 °C, respectively. Note that full densification cannot be obtained at 25 °C/min. But, the grey dotted curve demonstrates that the densification is completed at 1450 °C with lower heating rate (2 °C/min). Concerning the results of microwave sintering, the first significant outcome of Fig. 7 is that the density of a microwave-sintered material is larger than the density of a material conventionally sintered at the same measured temperature (in the case of microwave sintering tests, the temperature of the upper surface of the specimen). For direct microwave-sintered specimens, the final relative densities are 95.1%, 95.0% and 96.8% at 1275 °C, 1360 °C and 1500 °C, respectively. The hybrid microwave-sintered materials heated to 1200 °C, 1275 °C and 1340 °C have relative densities of 81.7%, 90.5% and 95.8%, respectively. All these values are significantly higher than the values expected for materials conventionally sintered at comparable temperatures. Besides, when the hybrid microwave sintering at 1350 °C was followed by a dwelling time of 1 h, the final density increased sharply from 95.8% to 98.6%. In the particular case of very fast hybrid microwave sintering, the final density was about 87% at 1225 °C.

3.2. Microstructure

The microstructure of the sintered materials has been observed by SEM in longitudinal sections along the axis of the cylindrical samples. As expected, the conventional-sintered specimens exhibit a homogeneous microstructure made of equiaxed grains with an average size of 220 nm at 1360 °C and 430 nm at 1550 °C (Fig. 8). In the specimens sintered by direct microwave heating (tests D3, D4 and D5), the grains are smaller in the top section (in average, 200 nm at 1275 °C, 240 nm at 1360 °C and 385 nm at 1500 °C), and larger in the central and bottom sections (in average, 240 nm, 260 nm and 435 nm, at 1275 °C, 1360 °C and 1500 °C, respectively), as shown in Fig. 9 for specimens D3 and D5.

In contrast, the microstructure of the hybrid microwave-sintered material heated at 1340 °C (test H8) can be considered as homogeneous, since the average grain size is 215 nm in the upper zone, 225 nm in the central and 230 nm in the bottom zone (Fig. 10). These values are close to the 220 nm average

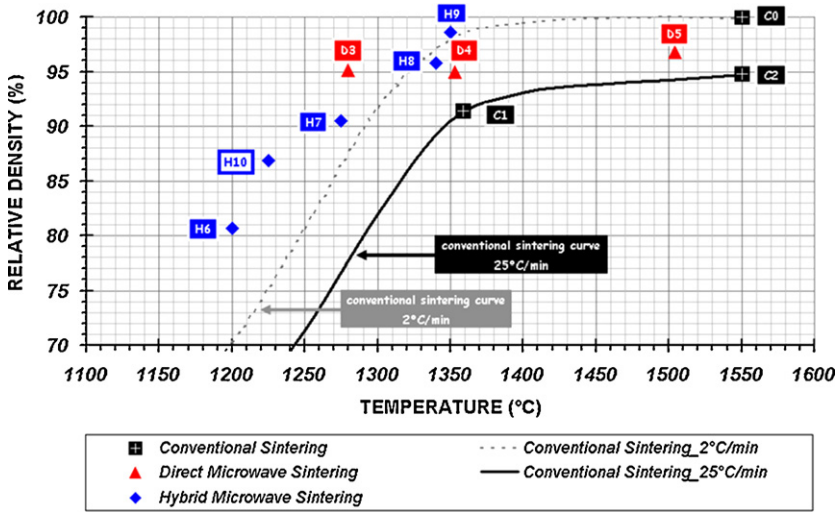

Fig. 7. Variation of the final relative density vs. maximal temperature for conventional (C), direct microwave (D) and hybrid microwave (H) sintering tests.

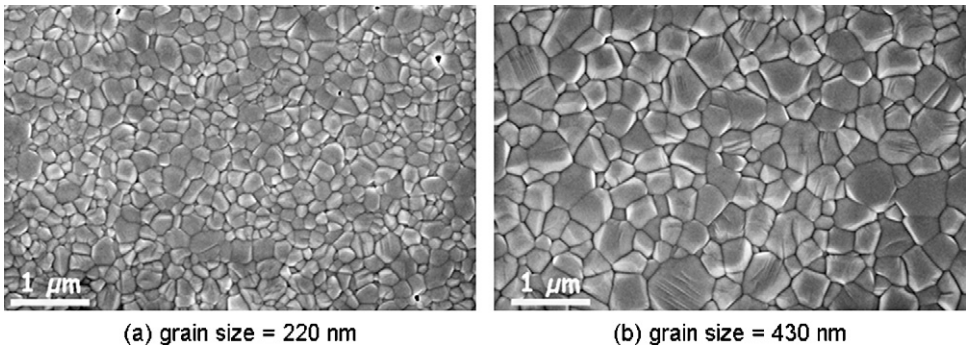

Fig. 8. SEM micrographs of specimens conventionally sintered at two temperatures. Thermally etched polished sections: (a) C1—1360 °C and (b) C2—1550 °C.

grain size of the specimen conventionally sintered at 1360 °C, which is less dense (91.4%) than the hybrid one (95.8%). When the specimen has been maintained during 1 h at 1350 °C (test H9), in comparison with the previous case, the sintered material exhibits an average grain size slightly larger in the central zone (Fig. 10: 270 nm instead of 220 nm) but close in the bottom and top zones (230–240 nm instead of 210–230 nm). Finally after fast sintering at 1225 °C (test H10), the average grain size was in the 140–250 nm range.

3.3. Sintering temperature–final density–grain size

In Fig. 11, the average grain size measured in the top, central and bottom zones for all sintered specimens are reported

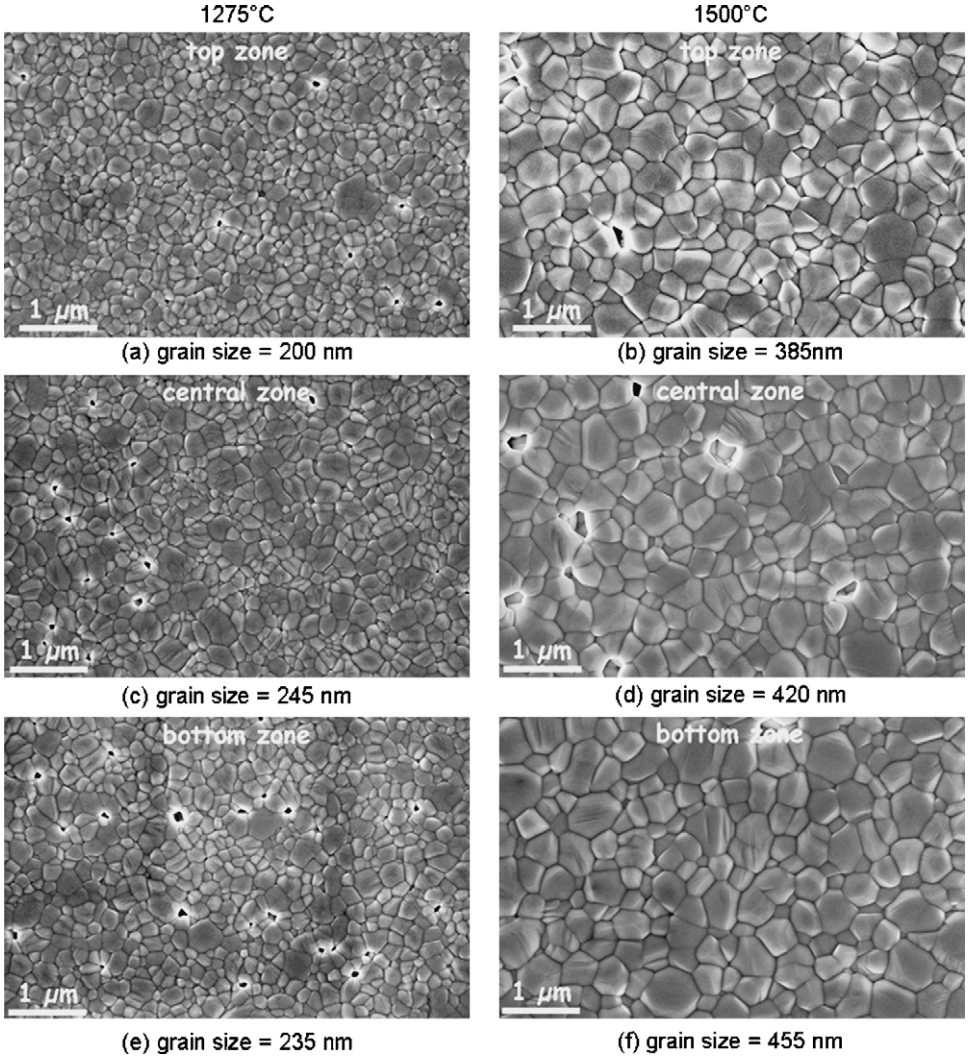

Fig. 9. SEM micrographs of the materials obtained by direct microwave sintering at two temperatures: D3 (left)—1275 °C and D5 (right)—1500 °C. Microstructures of the top (a and b), central (c and d) and bottom (e and f) zones of the specimens.

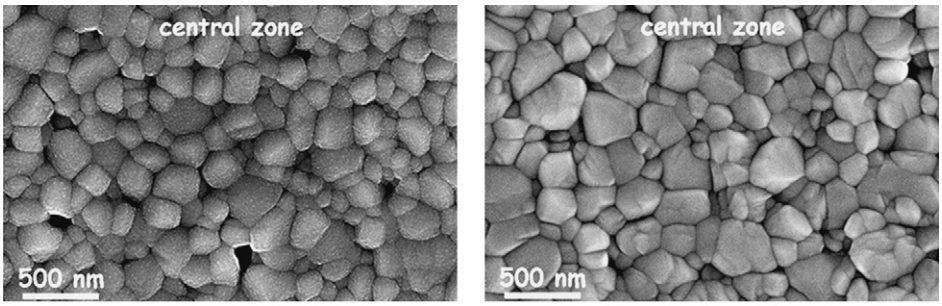

Fig. 10. SEM micrographs of materials obtained by hybrid microwave sintering (a) H8 (95.8%)—1340 °C (0 h) and (b) H9 (98.6%)—1350 °C (1 h).

as function of (a) the relative final density and of (b) the maximal sintering temperature. The classical representation of the grain size changes as function of density (sintering path[20,21]) shows that the microstructure is always finer in microwave-sintered specimens for a given density. Conventional sintering results in homogeneous microstructure and particularly slow grain growth in the final stage of sintering (C2 → 430 nm and C0 → 450 nm); whereas microwave-sintered specimens exhibit a fairly heterogeneous microstructure, especially after direct microwave sintering. The finest average grain sizes were always measured in the upper zones. These data confirm the previous SEM micrographs observations. The second graph (Fig. 11b)

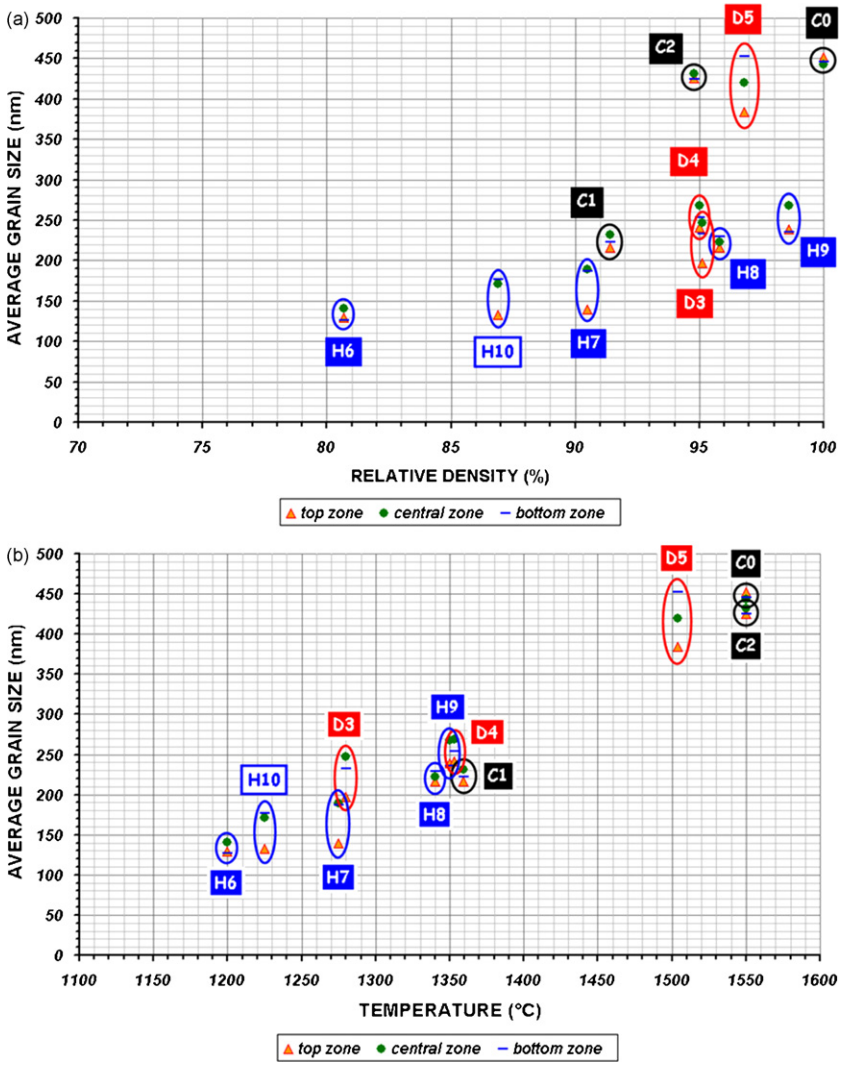

Fig. 11. Variation of the average grain size in the top, central and bottom zones vs. (a) the final relative density and (b) the sintering temperature for conventional (C), direct microwave (D) and hybrid microwave (H) sintering tests.

indicates that the main parameter governing grain growth is the maximal sintering temperature. In this representation there is no specific effect of the heating rate, of the dwelling time and of the heating mode on the grain size.

4. Discussion

The main goal of this study was a comparison of microwave heating and conventional sintering for a nanometric zirconia powder in terms of densification and microstructure changes. For this purpose, an intermediate heating rate of 25 °C/min, which could be followed in both cases, was chosen: it means fast heating for conventional sintering but relatively slow heating for microwave processing.

The results obtained by conventional sintering will first be discussed. Zirconia compacts got to 91.4% relative density and 220 nm grain size at 1360 °C and 94.8% and 430 nm at 1550 °C for conventional sintering at 25 °C/min. The final microstructure was homogeneous in spite of the relatively high heating rate. In fact, the external surface of a conventionally sintered compact is heated by radiation and by convection and heat is conveyed by conduction from the surface to the core of the sample. Thus, temperature should be higher close to the surface than in the core. However, for small samples subjected to standard heating rates, the effect of this gradient can be neglected and a homogeneous microstructure is classically observed. With a 2 °C/min heating rate up to 1550 °C, the density increased to 100% but the final grain size was only 450 nm. Thus, the conventional sintering experiments evidence a significant effect of the heating rate on the densification behaviour: a slower heating rate results in a higher final density. However, the grain size is not modified if the maximal temperature remains unchanged. This means that keeping the material longer at high temperature does not affect grain growth.

Microwave processing involves a different heating behaviour since heat is produced in the bulk of the compact and escapes through the external surfaces by radiation and convection. Therefore, an inverse thermal gradient takes place, with a higher temperature in the core than at the surface. Thermal insulation of the specimen is required to reduce thermal losses and thus decrease temperature gradients. Moreover, in our device the insulation of the upper part is incomplete because we need to keep a hole for temperature measurement. Thus the temperature measured by the IR camera is certainly lower than the temperature in the core of the specimen.

Susceptor-assisted microwave sintering is of course more delicate. Assuming that the susceptor did not shield the compact from the microwaves despite its high absorbing capacity, our observations suggest that, at least above 600 °C, the specimen is heated both upon its surface by radiance from the susceptor and in its bulk by coupling with the microwave. To validate this hypothesis, we estimated the penetration depth of microwaves in SiC with the classical equations of electromagnetic theory. The main issue was to choose a realistic value for the dielectric parameters of our SiC material, which cannot be measured. The values that are available in the literature are rather dispersed. Moreover it is very likely that these parameters depend on the microstructure of the material. We found that the penetration depth might vary between a few mm and a few cm, depending on the chosen values. As the thickness of our susceptor is 5 mm, the assertion that the specimen inside the susceptor is exposed to microwaves is not extraneous.

As shown in Fig. 7, for a given sintering temperature, both direct and hybrid microwave-sintered materials reached larger final densities than those of the conventionally sintered materials. The microstructure was found to be quite homogeneous in the hybrid microwave-sintered specimens. Fig. 11b shows a significant increase of the grain size with increasing temperature in the 1200–1500 °C range, before the occurrence of a sluggish grain growth phenomenon. This shows that the temperature measured on the specimen top surface is representative of the bulk temperature. It means that the SiC susceptor acts as an efficient insulation system. In comparison with the sample conventionally sintered at 1360 °C, the sample sintered with the hybrid mode at 1340 °C exhibited a much higher density (95.8% against 89%), whereas its grain size was similar (210 nm against 220 nm). The improvement of densification is even stronger at lower temperatures: 90.5% against 77% at 1275 °C and 81% against 63% at 1200 °C. The final density significantly increased to 98.6% after a 1 h soaking time at 1350 °C, whereas the grain size showed a slight growth from 210–230 nm to 230–270 nm. This result confirms a conclusion drawn from conventional sintering tests: the grain size is mainly related to the maximal temperature and is not significantly influenced by the thermal cycle. Moreover, our data showing similar grain sizes in conventionally and microwave-sintered materials at the same density suggest that the microwaves had no direct effect on cation segregation at the grain boundaries during the phase partitioning process, which is known to be responsible for the sluggish grain growth during the final stage of sintering.[25]

In contrast with hybrid microwave sintering, direct microwave sintering resulted in microstructure gradients depicted by grain size measurement. Although this measurement was biased by thermal etching, we presume that the grain size differences give relevant information about temperature gradients. This assumption is strengthened in Fig. 11b, which shows a rational variation of grain size vs. temperature. Thus, larger grain size in the bottom and central zones of the specimens should indicate a larger temperature in these zones than the temperature measured on the top surface. This thermal gradient is a consequence of the lack of insulation of the top surface combined with the aforementioned inverse gradient induced by microwave heating. The grain size measured in the upper zone of the microwave-sintered specimens at 1360 °C (D3 test) is almost the same as the one measured in the bottom zone of the microwave-sintered specimens at 1275 °C (C1 test). Therefore, assuming that the grain size depends on the sintering temperature, the temperature difference between the central and bottom zones and the upper surfaces of D3 specimen can roughly be estimated at 80 °C (see Fig. 11b). The same reasoning applied to D5 and C1 tests leads to a temperature difference of 50 °C in D5 specimen. This order of magnitude of the thermal gradient has been confirmed by the results of finite element simulation

of microwave heating in a single-mode cavity.[26] In any case, we found once again that all microwave-sintered specimens exhibited a larger final density than the final density of conventionally sintered samples at the same temperature (Fig. 7). This gain in densification was more significant at lower temperature: at 1275 °C the specimen D3 reached a relative density of 95% compared to only 79% in conventional sintering. A reasonable interpretation for this positive microwave effect on the densification of the material in the early stage of sintering is that the oscillating electric field enhances the interface reaction defect formation proposed by Bernard-Granger and Guizard[21] as the limiting mechanism at low relative density and for small grain size.

Finally, we demonstrated that very fast microwave sintering with a heating rate higher than 200 °C/min was feasible in our microwave furnace. However it was impossible to control accurately the prescribed thermal cycle and the final microstructure was fine but heterogeneous. In all likelihood, this is due to strong thermal gradients induced by high heating rate. Nevertheless, this experiment demonstrates the possibility to sinter such TZP materials at intermediate heating rates (between 25 °C/min and 200 °C/min). Most importantly, it shows that relative densities of 95–96% may be obtained without any crack.

5. Conclusion

Direct and susceptor-assisted microwave sintering experiments with 2 mol% yttria-doped zirconia powder compacts have been performed in a single-mode cavity at constant heating rate. This device included a thermal imaging camera measuring simultaneously the temperature of the top surface of the specimen and the temperature of the top surface of the susceptor. Using this device we achieved a fine control of the heating rate except for very high rates (>200 °C/min). In susceptor-assisted experiments with controlled heating rate, the temperature of the compact passes the temperature of the susceptor above 600 °C, which proved that the heating was really of the hybrid type. These hybrid microwave sintering experiments provided homogeneous specimens with a larger density but a similar microstructure as compared to the specimens conventionally sintered at the same temperature. In contrast, direct microwave heating tests led to materials with a slightly heterogeneous microstructure due to thermal gradients. However these materials are also much denser than the materials conventionally sintered at the same temperature.

To summarize, we evidenced a significant favourable effect of the electric field on the densification of 2 mol% yttria-doped zirconia nanopowder, particularly in the early sintering stage. Concerning microstructure changes, our results proved that the grain size was only dependent on the maximal sintering temperature, whatever the heating mode was. It means that the electric field does not accelerate grain growth in the final stage of sintering. However, due to the positive effect of microwaves on the densification, for the same relative density, a microwave heated specimen showed a smaller grain size as compared to the grain size achieved by conventional heating.

References

[1]. Kenkre VM. Theory of microwave interactions with ceramic materials. *Ceram Trans Am Ceram Soc* 1991;**21**:69–80.

[2]. Newnham RE, Jang SJ, Xu M, Jones F. Fundamental interaction mechanisms between microwaves and matter. *Ceram Trans Am Ceram Soc* 1991;**21**:51–67.

[3]. Sutton WH. Microwave processing of ceramic materials. *Ceram Bull* 1989;**68**(2):376–86.

[4]. Park SS, Meek TT. Characterization of ZrO_2–Al_2O_3 composites sintered in a 2.45 GHz electromagnetic field. *J Mater Sci* 1991;**26**:6309–13.

[5]. Tian Y-L. Practices of ultra-rapid sintering of ceramics using single-mode applicators. *Ceram Trans Am Ceram Soc* 1991;**21**:283–300.

[6]. Janney MA, Calhoun CL, Kimrey HD. Microwave sintering of oxide fuel cell materials. I. Zirconia–8 mol% yttria. *J Am Ceram Soc* 1992;**75**(2):341–6.

[7]. Clark DE, Sutton WH. Microwave processing of materials. *Annu Rev Mater Sci* 1996;**26**:299–331.

[8]. Nightingale SA, Dunne DP, Worner HK. Sintering and grain growth of 3 mol% yttria zirconia in a microwave field. *J Mater Sci* 1996;**31**:5039–43.

[9]. Nightingale SA, Worner HK, Dunne DP. Microstructural development during the microwave sintering of yttria–zirconia ceramics. *J Am Ceram Soc* 1997;**80**(2):394–400.

[10]. Upadhyaya DD, Ghosh A, Gurumurthy KR, Prasad R. Microwave sintering of cubic zirconia. *Ceram Int* 2001;**27**:415–8.

[11]. Wang J, Binner J, Vaidhyanathan B, Joomun N, Kilner J, Dimitrakis G, Cross TE. Evidence for the microwave effect during hybrid sintering. *J Am Ceram Soc* 2006;**89**(6):1977–84.

[12]. Xie Z, Li J, Huang Y, Kong X. Microwave sintering behaviour of ZrO_2–Y_2O_3 with agglomerate. *J Mater Sci* 1996;**15**:1158–60.

[13]. Mazaheri M, Zahedi AM, Hejazi MM. Processing of nanocrystalline 8 mol% yttria-stabilized zirconia by conventional, microwave-assisted and two-step sintering. *Mater Sci Eng* 2008;**A492**:261–7.

[14]. Binner J, Annapoorani K, Paul A, Santacruz I, Vaidhyanathan B. Dense nanostructured zirconia by two stage conventional/hybrid microwave sintering. *J Eur Ceram Soc* 2008;**28**:973–7.

[15]. Goldstein A, Travitzky N, Singurindy A, Kravchik M. Direct microwave sintering of yttria-stabilized zirconia at 2.45 GHz. *J Eur Ceram Soc* 1999;**19**:2067–72.

[16]. Wilson J, Kunz SM. Microwave sintering of partially stabilized zirconia. *J Am Ceram Soc* 1988;**71**(1):C-40–1.

[17]. Fujitsu S, Ikegami M, Hayashi T. Sintering of partially stabilized zirconia by microwave heating using ZnO–MnO_2–Al_2O_3 plates in a domestic microwave oven. *J Am Ceram Soc* 2000;**83**(8):2085–7.

[18]. Zhao C, Vleugels J, Groffils C, Luypaert PJ, Van Der Biest O. Hybrid sintering with a tubular susceptor in a cylindrical single-mode microwave furnace. *Acta Mater* 2000;**48**:3795–801.

[19]. Chen I, Wang X-H. Sintering dense nanocrystalline ceramics without final-stage grain growth. *Nature* 2000;**404**:168–71.

[20]. Mazaheri M, Simchi A, Dourandish M, Golestani-Frad F. Master sintering curves of a nanoscale 3Y-TZP powder compact. *Ceram Int* 2009;**35**:547–54.

[21]. Bernard-Granger G, Guizard C. Apparent activation energy for the densification of a commercially available granulated zirconia powder. *J Am Ceram Soc* 2007;**90**(4):1246–50.

[22]. Stoto T, Nauer M, Carry C. Influence of residual impurities on phase partitioning and grain growth processes of Y-TZP materials. *J Am Ceram Soc* 1991;**74**(10):2615–21.

[23]. Colomban Ph, Badot JC. Le chauffage par micro-ondes: méthode de cuisson des céramiques en 1990! *L'Industrie Céramique* 1979:275.

[24]. Willert-Porada M, Gerdes T, Metalorganic. Microwave processing of eutectic Al_2O_3–ZrO_2 ceramics. *Mater Res Soc Symp Proc* 1994;**347**:563–9.

[25]. Matsui K, Yoshida H, Ikuhara Y. Isothermal sintering effects on phase separation and grain growth in yttria-stabilized tetragonal zirconia polycrystal. *J Am Ceram Soc* 2009;**92**(2):467–75.

[26]. Bouvard, D., Charmond, S., Carry, C.P., Finite element modelling of microwave sintering, *Ceram. Trans.*, 2010; **209**.